Geosciences and Geological and Petroleum
Engineering Faculty Research & Creative Works

Geosciences and Geological and Petroleum
Engineering

01 Sep 2005

Active-Passive Array Surface Wave Inversion and Comparison to Borehole Logs in Southeast Missouri

Alexei A. Malovichko

Neil Lennart Anderson
Missouri University of Science and Technology, nanders@mst.edu

Dmitriy A. Malovichko

Denis Yu Shylakov

et. al. For a complete list of authors, see https://scholarsmine.mst.edu/geosci_geo_peteng_facwork/153

Follow this and additional works at: https://scholarsmine.mst.edu/geosci_geo_peteng_facwork

Part of the Geology Commons

Recommended Citation

Active-passive Array Surface Wave Inversion and Comparison to Borehole Logs in Southeast Missouri

Alexei A. Malovichko[1], Neil L. Anderson[2], Dmitriy A. Malovichko[3], Denis Yu. Shylakov[3] and Pavel G. Butirin[3]

[1]Geophysical Survey of Russian Academy of Sciences, 189, Lenin Av., Obninsk, Kaluga district, 249035, Russia
Email: amal@gsras.ru
[2]Department of Geology and Geophysics, University of Missouri-Rolla, Rolla, Mo., 65401
Email: nanders@umr.edu
[3]Mining Institute, Ural Branch, Russian Academy of Sciences; 78a, Sibirskaya St., Perm, 614007, Russia
Email: mal@mi-perm.ru

ABSTRACT

In May 2002, both active- and passive-source surface wave data were acquired using 4-channel arrays at six selected bridge sites in southeast Missouri. Processing of acquired data (increase of signal-to-noise ratio, estimation of phase velocities) was carried out and dispersion curves of Rayleigh wave phase velocities were constructed. Each fundamental mode dispersion curve was then inverted by linearised optimization to a layered shear-wave velocity profile to depths of up to 60 m.

The estimated shear-wave velocity profiles were compared to other geotechnical data that had been previously acquired at each test site for the Missouri Department of Transportation (MoDOT) including cone penetrometer test (CPT) data, borehole lithologic control, seismic cone penetrometer test (SCPT) shear-wave data and cross-borehole (CH) shear-wave data. The surface wave models, although smoother than the destructive test logs, are accurate and consistent (17% average difference with CH results on two sites), and, moreover, provide information on lithology above the water table and at depths beyond the SCPT and CH limitations, in a more logistically-easier and cost-effective manner.

Introduction

Information about the in situ shear modulus of soils at bridge sites is critically important for the evaluation of foundation integrity. This is particularly true in terms of assessing the soil's response to strong ground motion. A wide variety of field techniques and tests are available for the estimation of the shear modulus of soils. There are several seismic methods which involve the measurement and interpretation of waveforms at different points on the earth's surface and represent non-invasive and non-destructive field techniques.

The Spectral Analysis of Surface Wave (SASW) technique, introduced by Nazarian *et al.* (1983), is a seismic method that uses the dispersive characteristics of Rayleigh-type surface waves to determine the variation of the shear-wave velocity of layered systems with depth. The SASW method and its analogs (MASW and others; Park *et al.,* 2000) are very attractive due to relatively low acquisition, processing and interpretation costs. SASW data can also be acquired in areas inaccessible to drill rigs and at depths or in soils that cannot be tested using conventional SCPT technologies. On the other hand, field acquisition parameters are target and site specific. Additionally, the processing of SASW data is not always straight forward because surface wave phase velocities are connected to the shear modulus of layered strata in a complicated manner.

In May 2002, a geophysics crew consisting of scientific researchers from the University of Missouri-Rolla (USA) and the Mining Institute of Perm (Russia) tested a modification of the SASW method at six bridge sites in southeast Missouri (Fig. 1). Surface wave phase velocities were determined from the analysis of square array field data obtained during both "active" seismic testing and "passive" seismic monitoring. These phase velocities were inverted and used to generate vertical shear-wave velocity profiles with maximum depths in the order of 60 m. The estimated shear-wave velocity profiles were compared to other geotechnical data provided by MoDOT, including SCPT and CH shear-wave velocity profiles, and lithologic control derived from both borehole sampling and CPT testing.

Basic Principles Surface Wave Methods

The surface wave method uses the dispersive characteristics of surface waves (Rayleigh waves in this case) to determine how the shear-wave velocity of a layered subsurface varies with depth. This method generically comprises three main stages:

Stage 1: Field Measurements

Rayleigh wave data can be acquired using active and/or passive methods. In the active method an artificial
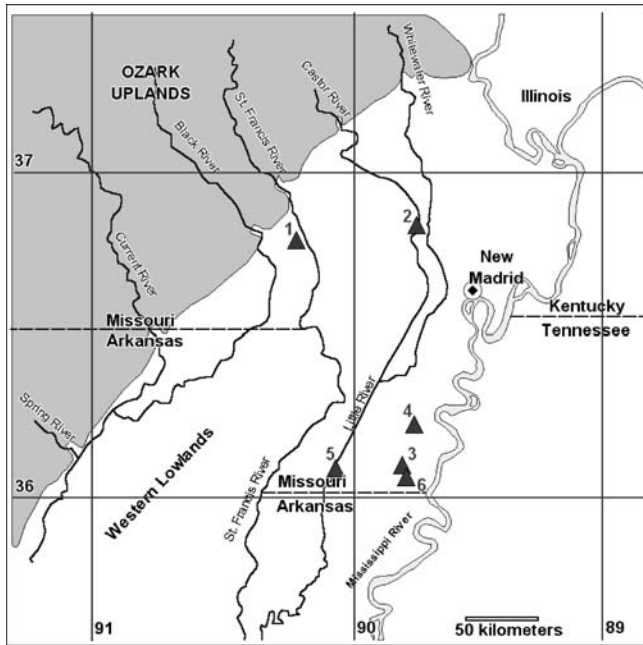
Figure 1. Map of southeast Missouri showing location of six SASW test sites: #1: A-3709 bridge; #2: A-5648 bridge; #3: L-472 bridge; #4: A-1466 bridge; #5: L-302 bridge; #6: A-5460 bridge.

impulsive or vibrating seismic source is used to generate higher frequency Rayleigh waves, which are recorded using a linear array of ground-coupled, low-frequency geophones. In the passive method, lower-frequency seismic waves arising from microtremors and/or urban (traffic) noise are recorded using two-dimensional arrays of geophones (Zywicki and Rix, 1999; Liu *et al.*, 2000). The use of geophone arrays allows phase velocities of wave trains to be determined simultaneously with the direction to their source. However, as shown by Louie (2001), even a linear geophone array can be used. But it demands special processing of the acquired data. It is generally assumed in the passive method that the fundamental mode of Rayleigh waves prevails on the field-recorded waveforms. Other types of seismic waves, including body waves and higher modes of Rayleigh waves are also recorded, however these are considered as noise.

The combination of active and passive methods has these advantages.

— the active method can provide high-quality Rayleigh-wave dispersion data in a relatively high-frequency range, so we obtain accurate constraints on near-surface layer velocities.
— the passive method is favorable for resolution of longer wavelengths, which contain information about deeper layers.

In conventional SASW, two receivers are used, either expanded about a common midpoint or common receiver

point to measure progressively larger wavelengths. We will show by a modified array SASW method, variation of source azimuth and offset relative to an array provides a smoother, path averaged dispersion curve.

Stage 2: Processing the Data to Obtain the Observed Dispersion

In the active method, the Rayleigh wave dispersion curves are generated on the basis of the analysis of the phase spectra of recorded waveforms from various source near-offsets and geophone spacings. In the passive method, frequency-wavenumber analysis can help to extract information about coherent wave packets passing through an array of geophones. The output of processing is a dispersion curve, which is the phase velocity vs. frequency relationship of a given mode(s) of Rayleigh waves.

## Stage 3: Inversion of Observed Dispersion to a Shear-wave Velocity Profile

Inversion represents the estimation of the vertical shear-wave velocity profile that best matches the Rayleigh wave dispersion curve. Usually, only shear-wave velocity is inverted for (not compressional-wave velocity or density) as the Rayleigh wave dispersion curve is most sensitive to this parameter. There are two main inversion strategies: global search and local search. Global-search procedures sample a broader model space and can easily incorporate any number of parameters (*e.g.,* layer thicknesses) but require more iterations than local search procedures, which iteratively improve the likelihood of the shear-wave velocity profile based on linearity about an initial estimate.

Field Procedures

Field measurements were conducted using the Russian mobile seismic station "ISK-2" and an array of seismological geophones (model SM3-KV). These geophones represent broadband electromagnetic pendulum vertical velocity transducers. They have a flat response characteristic over the frequency range 0.7–40 Hz (Fig. 2) and enable the recording of displacements in the range 10^{-9}–5.10^{-3} m.

Active-source Modified SASW

Active Rayleigh wave data were generated at all bridge sites using both a track-mounted Bison EWG weight drop source and a sledge hammer source. Unlike conventional SASW, which usually employs a source and two receivers in a linear arrangement, we employ a "modified SASW," where Rayleigh waves were recorded using 4-geophone square arrays (network). The size of the rectangular side was varied on every site in the range 5 m to 50 m. The larger spacing between geophones was used for longer source-geophone offsets and the smaller for shorter offsets. The Bison unit generated higher-amplitude Rayleigh waves and
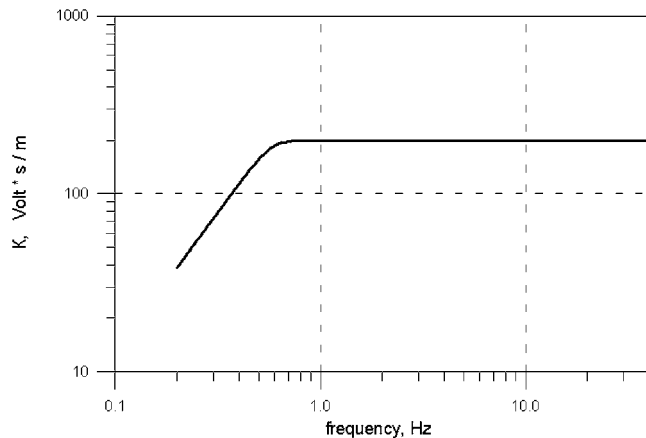
Figure 2. Gain-frequency characteristic of geophone SM3-KV.

was employed when the source was more than 50 m from the nearest geophone. The sledge hammer source generated lower-amplitude Rayleigh waves and was employed when the source was less than 50 m from the nearest geophones and very often in areas inaccessible to track-mounted weight drop. Multiple active-source Rayleigh wave records were generated at each site. The measurements were repeated for different azimuths of source relative to the array.

Figure 3 illustrates segments of seismograms obtained at two different bridge sites using the Bison unit as a source of seismic signals. Noise levels were low at Bridge Site #6 (RMS noise amplitude is near 1 μm/s) and well-defined Rayleigh waves at near offset distance of 90 m. The level of traffic noises at Bridge Site #2 was high (RMS noise amplitude is near 40 μm/s), so it was rather difficult to select useful signal from recorded data.

For any given array, we usually fired 20 to 100 times, each shot on average about 5 seconds apart, to ensure the entire dispersive wave train was measured, while recording continuously.

The typical waveforms of signals generated using a sledge hammer source and a Bison EWG weight drop source and their amplitude spectra are presented in Fig. 4. As illustrated in Fig. 4, these active sources generate relatively high-frequency Rayleigh waves (6–30 and 6–20 Hz, respectively).

Passive Array Measurements

Passive seismic data were also acquired at all bridge sites. The arrays with maximum size 50 m were used. The time of the continuous recording was 20–30 minutes. We suppose that traffic or vibrating mechanism were the primary source of the recorded passive Rayleigh waves. These passive sources generated Rayleigh waves with measurable frequencies as low as 3 Hz.

Data Processing

Passive-source Rayleigh wave data were used to generate lower-frequency phase velocity curves (in the range 3–12 Hz) at each bridge site. The largest wavelength obtained there was 220 m. Active-source Rayleigh wave data were used to generate higher-frequency phase velocity curves (in the range 7–20 Hz). Even with a maximum geophone spacing of 50 m, the active measurements only allowed wavelengths up to 50 m to be resolved. Two Rayleigh wave dispersion curves (passive and active) were combined during processing to form broader frequency-phase velocity curves (in the range 3–30 Hz) for each bridge site.

Active-source Modified SASW

The initial processing of active test data included two procedures: a) stacking of multiple signals generated for a
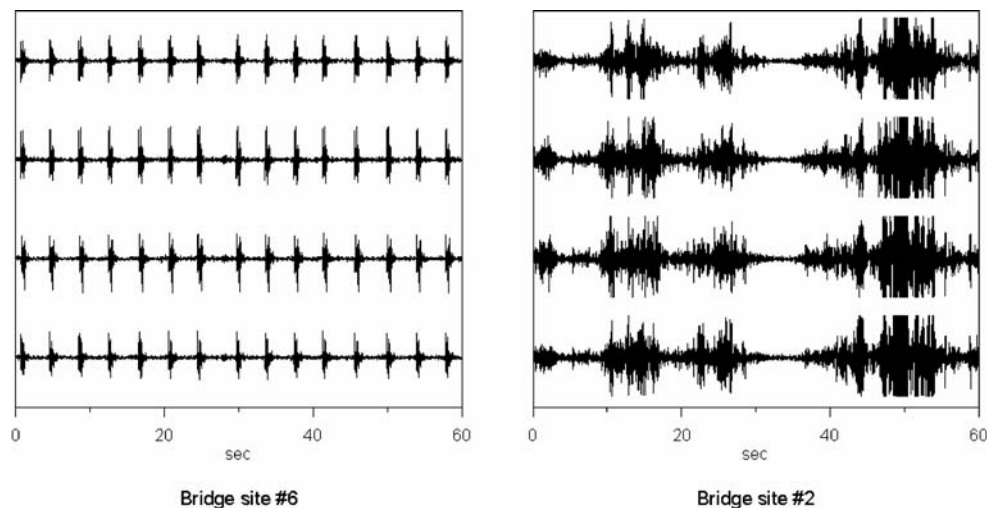
Figure 3. Fragments of seismograms at test sites with low (Bridge Site #6) and high (Bridge Site #2) levels of traffic noise.
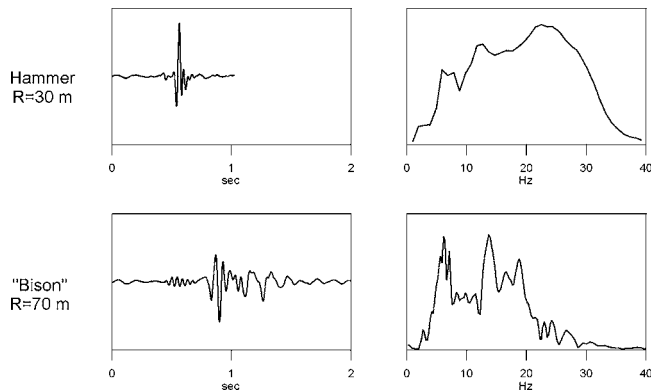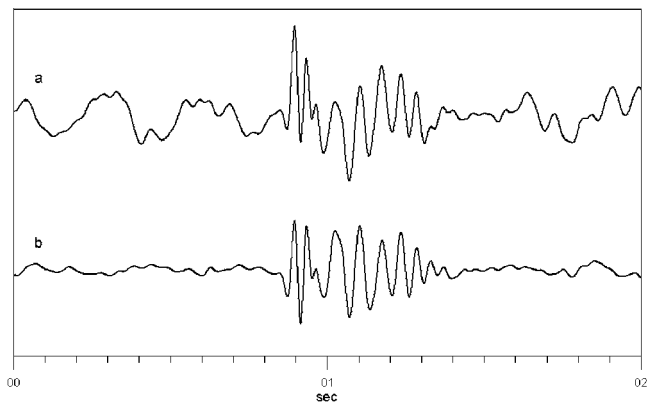
Figure 4. Typical waveforms for sledge hammer source and Bison source and their amplitude spectra.

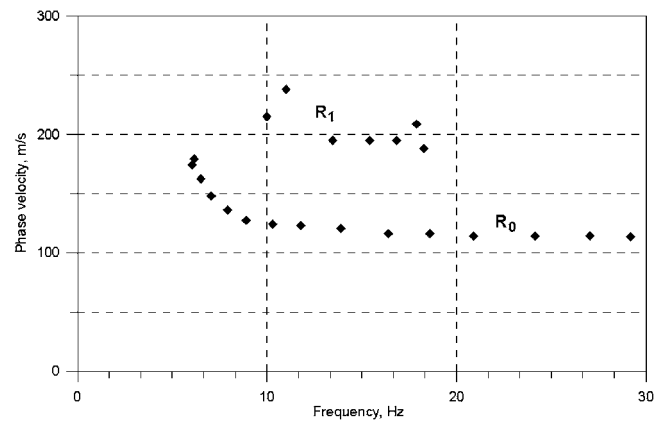**Figure 6.   Dispersion curves obtained from active monitoring at Bridge Site #5.**

constant source-array configuration and b) the construction of dispersion curve.

Field experience has shown that Rayleigh wave signals generated by multiple discharges of the same source for a constant source-geophone configuration exhibit significant resemblance, and that stacking can be effectively used to suppress of noises from different sources (traffic, etc.) thereby increasing the signal-to-noise ratio for Rayleigh waves. The stacking process is realized for each source-geophone configuration and for every geophone channel. It consists of the following steps.

- Identify and select a single superior signal (segment of relatively noise-free waveform with Rayleigh waves generated from single weight-drop or sledge hammer impact similar to shown on Fig. 5a).
- Calculate the cross-correlation function between the selected signal segment and entire waveform. Relative maximums on the cross-correlation function were considered to correspond to signal arrivals.
- Stack fragments of the entire waveform near calculated signal arrivals.

Figure 5.   Fragment of waveform with single signal from source (a) and corresponding stacked signal (b).

As a result more resolving signals were obtained (Fig. 5b) for each source-geophone configuration and for every geophone channel. These signals were used to construct the dispersion curve $\upsilon(f)$.

The existence of spherical wave front that passed all sensors of the array was implied in the course of $\upsilon(f)$ construction (*i.e.,* points source and 1D velocity model under the array were assumed). Estimation of phase velocities was realized by means of minimization of the functional

$$\sum_{i=1}^{4}\left[\upsilon(f)\frac{\varphi_i(f)-\varphi_{i+1}(f)+2\pi k_i}{2\pi f}-(d_i-d_{i+1})\right]^2,$$

where

$\varphi_i(f)$—value of phase spectra of the signal on the ith channel (for the sake of computation simplification the 1st channel was duplicated on the 5th channel)

d_i—distance from the source to the ith sensor

k_i—integer number taking into account possible phase turnovers between signals on ith and $(i + 1)$th channels.

During calculations different values of k_i (. . ., −2, −1, 0, 1, 2, . . .) were tested and as a result different variants of phase velocities $\upsilon(f)$ were obtained. The variant with minimal error was chosen.

Results of the described technique application to Bridge Site #5 data are presented on Fig. 6. Two dispersion curves ($\mathbf{R_0}$ and $\mathbf{R_1}$) are observed that could be interpreted as fundamental and 1st modes of Rayleigh waves.

Passive Array Measurements

Dispersion information was also recovered from the waveforms of microtremors recorded during passive monitoring (assuming microtremors were primarily fundamental mode Rayleigh waves induced by non-controlled sources such as traffic). The technique employed consisted of

Malovichko et al.: Active-passive Array Surface Wave Inversion
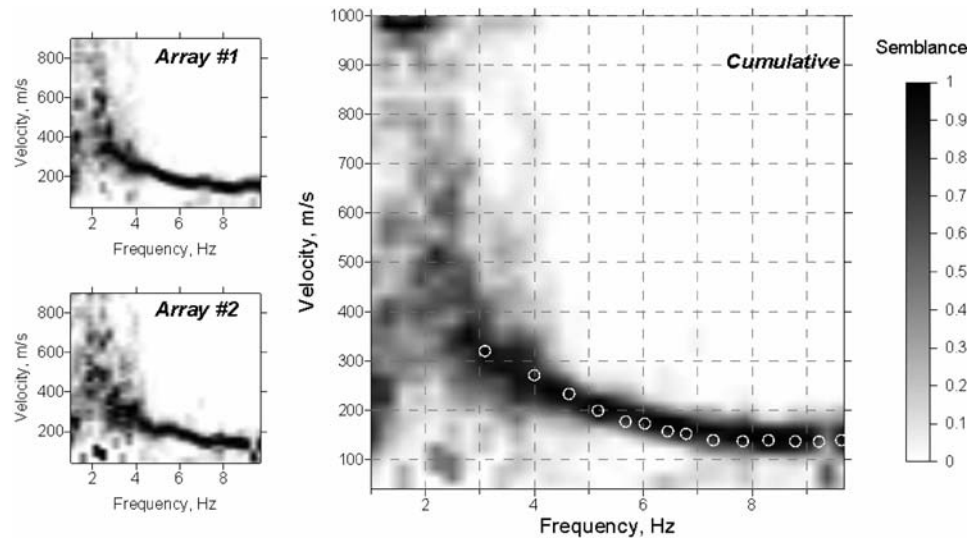
Figure 7.   Dispersion images obtained from passive monitoring at Bridge Site #5.

calculating and plotting semblance parameters for different frequencies and phase velocities of plane waves passing through the array. This technique is time-domain equivalent of the conventional frequency-wavenumber analysis. Certain maximums on the semblance plots were associated with Rayleigh waves. For illustration purposes, two semblance plots for Bridge Site #5 are depicted in Fig. 7. Array #1 data were acquired using a 27 m geophone spacing; Array #2 data were acquired using an 8 m spacing (Fig. 7). The fundamental harmonic dispersion curve in the interval 3–9 Hz is characterized by velocities in the 150–350 m/s range. These phase velocities correlate well in the high frequency range with dispersion data obtained during active

monitoring (Fig. 6). The combination of the dispersion data displayed in Fig. 6 and 7 were used to generate the composite dispersion curve of Fig. 8 (frequency range 3–20 Hz).

Inversion Algorithm

Shear-wave velocity inversion (re: SASW technique) is essentially the process of determining the shear-wave velocity profile $\beta(z)$ that best satisfies the calculated cumulative dispersion curve $\upsilon(f)$ and a priori information.

In the common case, phase velocities of surface waves are connected with medium parameters (density,
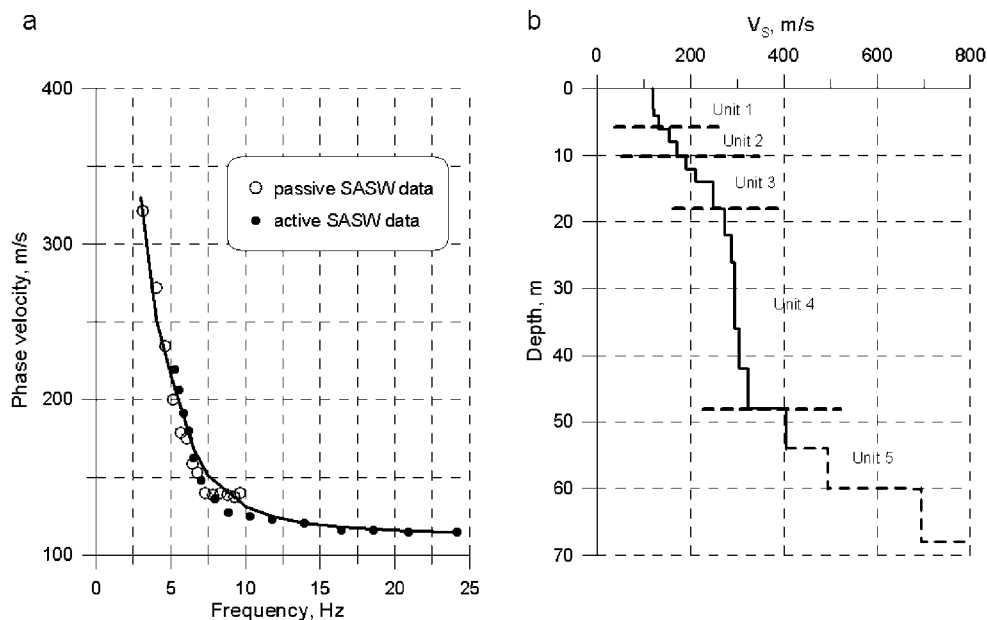
Figure 8.   Composite dispersion curves (a) and inverted vertical shear-wave velocity profile (b) for Bridge Site #5.

compressional-wave and shear-wave velocities) by non-linear functional dependencies:

$$\upsilon(f) = E(\beta(z)) \tag{1}$$

The form of E can be found in Aki and Richards (1980). The relation equation (1) can be transformed into a discrete form by approximating the medium (subsurface) as a set of M homogeneous beds with shear-wave velocities β_j ($j = 1, 2, \ldots, M$) and introducing vector $\overline{\beta}$ with length M where:

$$\overline{\beta} = [\beta_1, \ldots, \beta_M]^T.$$

The dispersion curve $\upsilon(f)$ over N frequencies ($f_1, \ldots, f_N$) can similarly be represented as vector $\overline{\upsilon}$ where:

$$\overline{\upsilon} = [\upsilon(f_1), \ldots, \upsilon(f_N)]^T.$$

Equation (1) can then be expressed in the form:

$$\upsilon_i = E_i(\overline{\beta}), \quad i = 1, 2, \ldots, N \tag{2}$$

We implemented the solution of nonlinear equation (2) by the Marquardt method (Aki and Richards, 1980) which consists of three iterative stages.

1. Obtaining the linear equations connecting the observed and target values: Equation (2) is linearized by Taylor expansion. The kth iteration approximate solution $\beta^{(k)}$ is:

$$\Delta\upsilon_i \approx F_{ij} \, \Delta\beta_j, \tag{3}$$

where $\Delta\upsilon_i = \upsilon_i - E_i(\overline{\beta^{(k)}})$, $\Delta\beta_j = \beta_j - \beta_j^{(k)}$ and $F_{ij} = \partial E_i / \partial\beta_j$. F represents a matrix of partial derivatives of phase velocities with respect to shear-wave velocities. We have used a variational algorithm for calculating the matrix F (as described by Aki and Richards, 1980) which is more stable than one used by Xia *et al.* (1999). Equation (3) sets rough linear joint between the correction to the velocity model $\Delta\overline{\beta}$ and the difference $\Delta\overline{\upsilon}$ between the observed and calculated values for the model $\beta^{(k)}$ dispersion curves.

2. Determination of correction to model: Taking into account the rough equation (3) correction, $\Delta\overline{\beta}$ is determined through the minimization of the functional

$$\Phi = |\Delta\overline{\upsilon} - F\Delta\overline{\beta}|^2 + \varepsilon^2|\Delta\overline{\beta}|^2, \tag{4}$$

where ε is damping factor, that decreases resolving power but increases the stability of the solution. Xia *et al.* (1999) recommend using ε values from 0.3 to 0.8 during computations. The next expression gives the minimum of Φ

$$\Delta\overline{\beta} = V(\Lambda^2 + \varepsilon^2 I)^{-1}\Lambda U^T \Delta\overline{\upsilon} \tag{5}$$

where

$F = U \Lambda V^T$ is the singular value decomposition (SVD) of partial derivatives matrix
I is the identity matrix

The SVD procedure was based on Press *et al.* (1992).

3. Insertion correction into model: The correction calculated by equation (5) is inserted in initial model for the kth iteration such that

$$\overline{\beta^{(k+1)}} = \overline{\beta^{(k)}} + \Delta\overline{\beta}.$$

The obtained model $\overline{\beta^{(k+1)}}$ is used as the initial one in the first stage of the next iteration. The described inversion algorithm is the similar to one of Herrmann (1996).

Results and Interpretation

The site-specific dispersion curves generated from field-acquired Rayleigh wave data were transformed into vertical shear-wave velocity profiles using the algorithm described above. Transformations were based on the following assumptions (Savich *et al.,* 1990), which satisfactory correspond to a great variety of soil situations:

- compressional-wave velocity to shear-wave velocity ratio α/β decreased from 3.0 (for shallowest layers, having depths less then 10 m) to 1.71 (for deepest layers, having depths more then 25 m);
- $\rho = 1.64 + 0.0008 \, \beta$, where ρ is density and β in m/s.

We did not analyze in detail the uniqueness of our inverted shear-wave profiles. The information about errors in dispersion curves was not used in the inversion. The shear-wave velocity model giving the best fit to an observed dispersion curve was regarded as the final solution. As a result a single shear-wave velocity profile was obtained for every site.

We now consider results of the combined active-passive array measurements and interpretations for bridge sites #5 and #4 in detail.

Bridge Site #5

The composite Rayleigh wave dispersion curves (observed values plotted as circles and theoretical values as a continuous line) and estimated vertical shear-wave profile from Bridge Site #5 are shown in Fig. 8. On the basis of average estimated interval shear-wave velocity, the SASW profile can be divided into five units: Unit 1 ($\sim$0–6 m; $\sim$120–140 m/s); Unit 2 ($\sim$6–10 m; $\sim$155–175 m/s); Unit 3 ($\sim$10–18 m; $\sim$190–250 m/s); Unit 4 ($\sim$18–48 m; $\sim$275–320 m/s); and Unit 5 ($>$48 m; $>$400 m/s). The division into units was made arbitrarily such that the layer velocity difference in the limits of the one unit did not exceed 15–30%.

Unit 1 (as per the STA 133+58 boring log supplied by MoDOT) correlates with a zone comprised mostly of moderately stiff to stiff clay with some sand layers (log depths $\sim$0–6 m); Unit 2 correlates with a zone comprised mostly of medium dense, gray sand with sparse gravel ($\sim$6–9 m); and
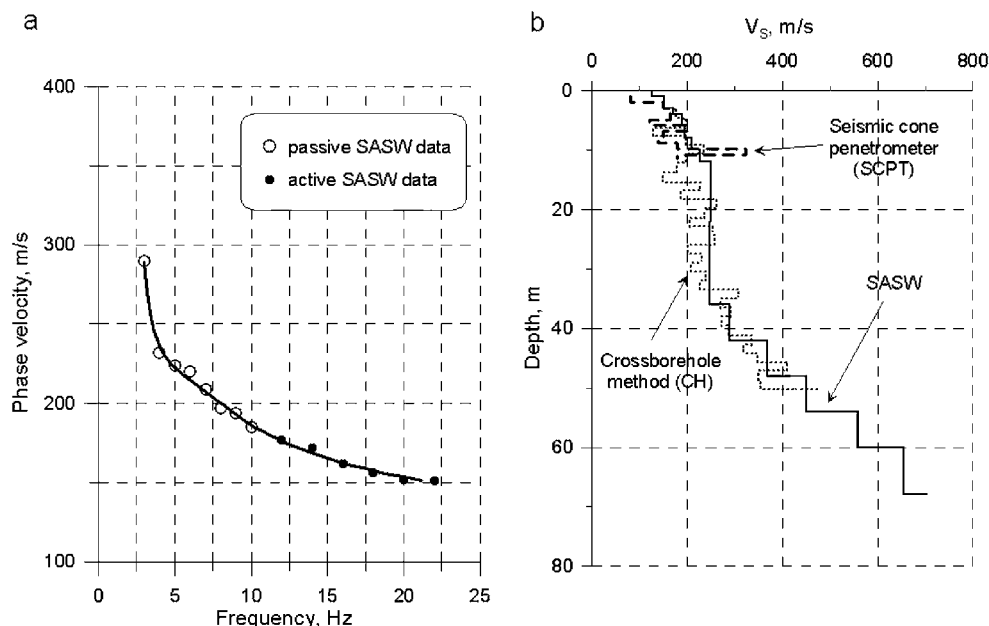
Figure 9. **Composite dispersion diagram (a) and shear-wave velocity profiles from various methods (b) for Bridge Site #4.**

Unit 3 and the top of Unit 4 correlate with a zone comprised of mostly dense to very dense, medium to coarse grained sand with some light gravel (~9 m to base of log at ~20 m). Unit 5 was not intersected at the Bridge Site #5 borehole location, however the general trend of the surface wave shear-wave velocity model also compared favorably with data acquired at the Bridge Sites #1 and #2 (not shown). At these locations, higher shear-wave velocities at progressively greater depths were associated with increasingly compacted sediment (predominantly sands). The surface wave models and lithological log data suggest a near-direct correlation between Vs and soil type.

Bridge Site #4

Shear-waves velocity profiles for Bridge Site #4 (Fig. 1) are presented as Fig. 9. The different curves represent results obtained by the combined active-passive array method, the cross borehole method (BH), and trial of the seismic cone penetrometer test (SCPT).

On the basis of average estimated interval shear-wave velocity, the SASW profile can be divided into six units: Unit 1 (~0–4 m; ~130–170 m/s); Unit 2 (~4–12 m; 190–230 m/s); Unit 3 (~12–43 m; ~250 m/s); Unit 4 (~43–48 m; ~370 m/s); and Unit 5 (>48 m; >460 m/s).

Unit 1 (as per B2 lithology log provided by MoDOT) corresponds with a zone comprised mostly of brown, sandy silt to silty sand (borehole depths ~0–4 m); Unit 2 correlates with a zone comprised of gray, stiff to very stiff, sandy silt to silty sand (~4–11 m); Unit 3 correlates with a zone com-

prised of mostly dense to very dense fine sand (~11 m to base of borehole at ~31 m).

These results indicate there is a reasonable correlation between surface wave inverted shear-wave velocities and subsurface lithologies. The SCPT shear-wave velocities (Fig. 9) also appear to correlate reasonably well with both subsurface lithology and surface wave models. For example, the near-surface brown sandy silts and brown silty sands (<4 m depth) at the B2 site are characterized by SCPT shear-wave velocities ranging from ~160–200 m/s; the underlying stiff to very stiff sandy silts and silty sands are characterized by SCPT shear-wave velocities ranging from ~160–220 m/s.

The cross-borehole shear-wave velocity data acquired at vicinity of Bridge Site #4 are also presented in Fig. 9 (CH curve). Cross-borehole surveying used twinned boreholes separated by surface distance 4 m. These cross-borehole shear-wave seismic velocities correlate on average to within 17% with those derived from surface wave inversion.

More specifically, the surface wave model is characterized by shear-wave velocities that increase step-wise from about 130 m/s to 350 m/s. The same interval on the CH profile is characterized by shear-wave velocities that increase gradationally (with minor irregularities) from about 150 to 380 m/s. Note: the cross-borehole data acquired at Bridge Site #4 range in quality from poor to good. The quality of these data was adversely affected by the high volume of traffic on interstate I–55.

The surface wave models and lithological log data suggest a near-direct correlation between Vs and soil type.

Conclusions

Shear wave velocity models were inverted from array surface wave measurements at 6 bridge sites in Missouri. The combined active-passive procedure provided reliable shear-wave velocity profiles down to 60 m depth. Although smoother than destructive test logs, estimated models compare well with borehole derived measurements and provide information on lithology above the water table and at depths beyond the SCPT and CH limitations.

More specifically, surficial clays, described as silty, are characterized by shear-wave velocities ranging from ~90 m/s to 140 m/s. Clays described as containing sand are characterized by velocities ranging from ~120 m/s to ~170 m/s. Clayey silts to silty sands are characterized by velocities ranging from ~130 m/s to ~230 m/s, with sediments described as stiffer exhibiting characteristically higher velocities.

The surface wave inverted shear-wave velocities of sediments described as sand varied significantly at each bridge site, however there appears to be a very definite pattern to the observed velocity variations. The shear-wave velocities of sand increase almost monotonically (in a step-wise manner) with depth at each test site, suggesting that the shear-wave velocities of these unconsolidated sands are a function of depth of burial. In terms of sands with similar depths of burial, those described as dense to very dense exhibit relatively higher shear-wave velocities. The estimated shear-wave velocity profiles at Bridge Sites #2 and #4 (Fig. 9) correlates quite well with available cross-borehole shear-wave control (average difference 17%).

Acknowledgments

References

Aki, K., and Richards, P.G., 1980, Quantitative seismology: W.H. Freeman & Co., San Francisco, 932 p.

Herrmann, R.B., 1996, Computer Programs in Seismology: 3.0, Saint Louis University, Saint Louis, Missouri.

Liu, H.-P., Boore, D.M., Joyner, W.B., Oppenheimer, D.H., Warrick, R.E., Zhang, W., Hamilton, J.C., and Brown, L.T., 2000, Comparison of phase velocities from array measurements of Rayleigh waves associated with microtremor and results calculated from borehole shear-wave velocity profiles: Bulletin Seismological Society of America, **90**, 666–678.

Louie, J.L., 2001, Faster, better: Shear-wave velocity to 100 meters depth from refraction microtremor arrays: Bulletin of the Seismological Society of America, **91**, 347–364.

Nazarian, S., Stokoe, K.H., and Hudson, W.R., 1983, Use of spectral analysis of surface waves method for determination of moduli and thicknesses of pavement systems: Transportation Research Record, **930**, 38–45.

Park, C.B., Miller, R.D., and Xia, J., 1999, Multimodal analysis of high frequency surface waves: Proceeding of the Symposium on the Application of Geophysics to Engineering and Environmental Problems, 115–121.

Press, W.H., Teukolsky, S.A., Vetterling, W.T., and Flannery, B.P., 1997, Numerical Recipes in C. The Art of Scientific Computing: Cambridge University Press, 965 p.

Savich, A.I., Kuyndjich, B.D., and Koptev, V.I., 1990, Complex engineering and geophysical investigations during hydraulic structure construction. Nedra, Moscow, 462 p. (in Russian)

Xia, J., Miller, R.D., and Park, C.B., 1999, Estimation of near-surface velocity by inversion of Rayleigh waves: Geophysics, **64**, 691–700.

Zywicki, D.J., and Rix, G.J., 1999, Frequency-wavenumber analysis of passive surface waves: Proceeding of the Symposium on the Application of Geophysics to Engineering and Environmental Problems, 75–84.